

Numerical Optimization Strategy for Determining 3D Flow Fields in Microfluidics

A. Eden¹, M. Sigurdson¹, C. D. Meinhart¹, I. Mezić¹

¹University of California - Santa Barbara, Santa Barbara, CA, USA

Abstract

Introduction

Obtaining 3-dimensional measurements of fluid flows can be challenging. Current methods include expensive camera setups for 3D particle image velocimetry (PIV) or data-intensive 2D PIV experiments with algorithms to find out-of-plane components and generate 3D data [1]. Here we present a hybrid experimental-numerical method for generating 3D flow fields from 2D PIV experimental data and finite element simulations. An optimization algorithm is applied to a theory-based simulation of an alternating current electrothermal (ACET) micromixer in conjunction with 2D PIV data to generate an improved representation of the 3D steady state flow conditions. This data can be used to examine and assess mixing phenomena in such devices more accurately than would be possible through simulation alone. In addition, this hybrid method can be used to estimate unknown physical properties and offset uncertainties between experimental conditions and simplifying assumptions used to develop numerical models.

Use of COMSOL Multiphysics

Experimental conditions were simulated using COMSOL Multiphysics® software. A 3D component matching the design specifications of the micromixer was created and materials were assigned to specific domains according to (Figure 1b). Simulated physical equations were based on the theoretical model for ac electrothermal flows developed by Ramos et al in [2] and improved by Loire et al [3]. Built-in physics modules of "laminar single-phase flow" and "heat transfer in fluids" were used to solve the velocity and temperature fields, respectively, with the coupled governing equations from [3]. The "coefficient form PDE" module was used to solve the quasi-static electric field using the temperature-dependent electrical convection-diffusion equation from [3]. A Nelder-Mead optimization algorithm was used to achieve a better fit by minimizing the normalized mean square error between 2D PIV experimental velocity data, gathered in 4 different interrogation regions, and simulation results at the measurement plane.

Results

The optimization algorithm reduced the objective function, which was the square of the velocity normalized root mean square error (NRMSE), by a factor of 103. NRMSE values and control parameters for the original and optimized conditions are shown in (Figure 4), indicating a much

improved fit with the experimental data. The optimization drastically changed the simulated flow pattern to match the data, evident in (Figure 2f) and (Figure 3). Both the scale and direction of the optimized conditions match experimental results in (Figure 2d).

Conclusion

By applying this hybrid method, the normalized RMS velocity error between the simulation and experimental results was reduced by more than an order of magnitude. The optimization algorithm altered 3D fluid circulation patterns considerably, providing a more accurate representation of the 3D experimental flow field. Additionally, this method allowed us to scale and roughly estimate physical parameters to match experimental conditions. This experimental-numerical method shows promise in developing simulations that can more accurately reflect real experimental conditions, and can be generalized to a wide variety of flow problems.

Reference

[1] P Kauffman et al., Proper Orthogonal Decomposition based 3D microPIV: application to electrothermal flow study, 10th International Symposium on Particle Image Velocimetry, Delft, The Netherlands, July 1-3, 2013.

[2] A Ramos et al., Ac electrokinetics: A review of forces in microelectrodes, J. Phys. D: Appl. Phys 31 2338-53 (1998).

[3] S Loire et al., Ac electrokinetics: A theoretical and experimental study of ac electrothermal flows, J. Phys. D: Appl. Phys 45 185301 (2012).

Figures used in the abstract

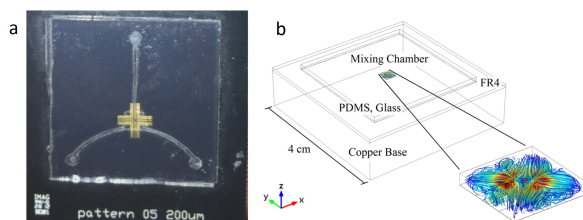


Figure 1: A top view of the ACET micromixer used in experiments, depicting the mixing chamber and patterned electrodes as well as the fluid inlets and microfluidic channels used to deliver the fluid solution to the chamber (a), and the modeled device with theoretical 3D streamlines for the optimized flow field (b).

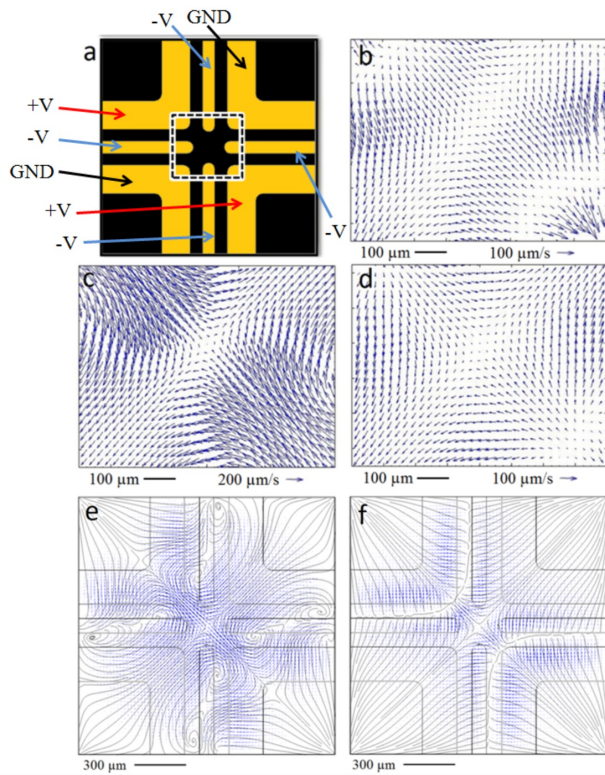


Figure 2: The electrode pattern with an overlay of the central interrogation region location (a), a top view of the fully processed PIV data from the central interrogation region (b), COMSOL simulation results of the 2D velocity field at the measurement plane for the original estimation of parameters (c), optimized COMSOL 2D velocity field at the measurement plane (d), original measurement plane flow pattern (e), and optimized measurement plane flow pattern (f). The optimized velocity field in (d) depicts regions of reversed flow in the top left and bottom right corners that are present in the PIV measurements but not in the original simulation. The optimized solution also has a much closer velocity magnitude to that of the PIV results in (b).

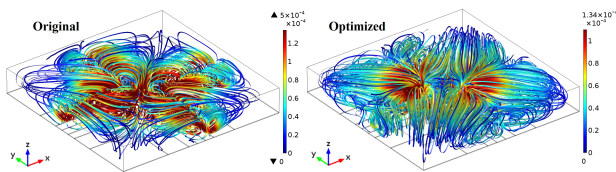


Figure 3: Colored 3D streamlines for the original non-optimized (left) and optimized (right) flow conditions in the mixing chamber, in m/s. While most of this 3D data is essentially extrapolated using a physical model, the optimization allows for a closer recreation of experimental flow conditions at the measurement plane, ultimately resulting in more accurate and useful out-of-plane flow information.

Parameter	Original	Optimized
Electrothermal Force Scaling	1	0.348
Electric Field Nonlinearity Scaling	1	3.125
Buoyancy Force Scaling	1	4.069
Dielectrophoretic Force Scaling	1	3.539
Fluid Thermal Conductivity	0.61 W m ⁻¹ K ⁻¹	0.104 W m ⁻¹ K ⁻¹
Fluid Electrical Conductivity	0.16 S/m	0.084 S/m
Fluid Dynamic Viscosity	9x10 ⁻⁴ Pa s	1.12x10 ⁻⁴ Pa s
Gaussian Function Width	5 μm	20 μm
Measurement Plane Location Offset	0	-48.25 μm
Center Electrode Width	200 μm	160 μm
Gap Width Between Electrodes	200 μm	205 μm
FR4 Thermal Conductivity, x-direction	0.8 W m ⁻¹ K ⁻¹	4.25 W m ⁻¹ K ⁻¹
FR4 Thermal Conductivity, y-direction	0.8 W m ⁻¹ K ⁻¹	3.26 W m ⁻¹ K ⁻¹
FR4 Thermal Conductivity, z-direction	0.3 W m ⁻¹ K ⁻¹	0.965 W m ⁻¹ K ⁻¹

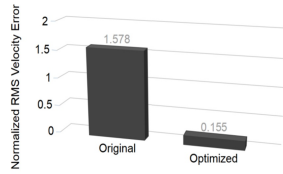


Figure 4: Optimization results, showing the original and optimized values of the chosen physical parameters (left) as well as the normalized RMS velocity error between the simulation results and PIV measurements for the central interrogation region (right), where $NRMSE =$

$\text{Objective}^{1/2}$. These results indicate that the relative error between the RMS velocity error and RMS velocity for the optimized results is only 0.155; that is, the optimized RMS error is less than 16% of the RMS velocity, compared to an RMS error nearly 160% of the RMS velocity for the non-optimized solution. Results from other interrogation regions showed similar reductions in error, indicating that the remaining regions of the velocity field at the measurement plane are also a much better fit with the experimental results.